Impact of gas cluster ion and accelerated neutral atom beam surface treatments on the laser-induced damage threshold of ceramic Yb:YAG

Contact *mariastefania.de-vido@stfc.ac.uk*

M. De Vido, K. Ertel, P. J. Phillips, P. D. Mason, S. Banerjee, J. M. Smith, T. J. Butcher, C. Edwards, C. Hernandez-Gomez, J. L. Collier

STFC Rutherford Appleton Laboratory, Central Laser Facility, Chilton, Didcot, OX11 0QX, UK

M. J. Walsh, S. Kirkpatrick, R. Svrluga

Exogenesis Corporation,

20 Fortune Drive, Billerica, MA 01821, USA

Abstract

We describe the application of the gas cluster ion beam (GCIB) and of the accelerated neutral atom beam (ANAB) surface treatments to ceramic Yb:YAG. We demonstrate that these techniques allow accurate control of ceramic Yb:YAG surface characteristics and constitute an alternative to conventional surface finishing techniques. In this study, we analyse the impact of angstrom level polishing and surface nano-texturing on laser induced damage threshold (LIDT) in the nanosecond pulsed regime of uncoated and antireflective coated ceramic Yb:YAG samples. We show that both techniques allow meeting the requirements on resilience to laser irradiation at fluence levels characterising high-energy laser systems. Moreover, we show that surface nano-texturing improves the LIDT of coated samples, possibly through an improvement in adherence of coatings to ceramic Yb:YAG substrates.

1. Introduction

Ultra-high intensity laser-matter interaction applications, such as particle acceleration [1, 2], intense X-ray generation [3] and inertial confinement fusion [4] require lasers operating at multi-J to kJ energy levels. Proof-of-principle demonstrations have so far been carried out using laser facilities relying on flash-lamp pumped amplifier technology, which severely limits both the repetition rate and the efficiency of such systems [5]. However, in order to achieve practicable real-world applications of laser-matter interactions in industrial, medical and scientific fields, lasers reliably and efficiently delivering nanosecond pulses at multi-Hz repetition rates with a lifetime of several billion shots are required. Diode-Pumped Solid State Laser (DPSSL) technology represents a promising approach which is currently being extensively investigated. Yb^{3+}-doped Yttrium Aluminium Garnet (Yb:YAG) in ceramic form has been identified as one of the most promising active media for high energy, high repetition rate DPSSL systems [6]. Currently, one important factor limiting the reliability of such laser systems is represented by laser-induced damage. In the nanosecond regime, laser-induced damage is caused by contamination or cracks which may affect optical coatings, substrates or interfaces between the two [7]. It has been demonstrated that such imperfections cause linear and non-linear absorption of high-intensity laser radiation, leading to unwanted damage growth [8]. Such issues have given a great impetus to the development of advanced material production and processing techniques. In this work, we propose the application of the Gas Cluster Ion Beam (GCIB) and the Accelerated Neutral Atom Beam (ANAB) treatments to process the surface of ceramic Yb:YAG. We demonstrate that GCIB is capable of producing nano-textured surface morphologies. Furthermore, we show that the combination of both GCIB and ANAB techniques allows achieving angstrom-level surface roughness, thus representing an alternative to established polishing techniques. We investigated the impact of both smoothing and nano-texturing capabilities on laser-induced damage resilience of ceramic Yb:YAG. To the best of our knowledge, this is the first time that the GCIB and the ANAB techniques have been exploited to treat the surface of optical ceramic Yb:YAG.

2. Method of Gas Cluster Ion Beam and Accelerated Neutral Atom Beam

As described in a previous publication [9], the GCIB technique, first proposed by Kyoto University, employs intense collimated beams of ionised gas clusters to achieve highly controllable surface finishing. The ANAB technique [10], recently developed by Exogenesis Corporation, converts the energetic gas cluster ions produced by the GCIB technique into intense collimated beams of neutral gas atoms with controllable average energies between 10 eV and a few hundreds of eV. A standard GCIB setup uses pressurised argon gas which is expanded into vacuum using a nozzle to form atom clusters comprised of a few hundreds to a few thousands atoms. Gas clusters are made positively charged by electron impact ionization and are subsequently accelerated through a high potential before reaching a target at ground potential. Additional beamline components allow precise control and focusing of the cluster beam. A modified GCIB configuration, enabling the production and the utilisation of a neutral atom beam instead of a gas cluster beam, is shown in Fig. 1. Main modifications with respect to a GCIB setup consist of an electrostatic deflector to remove ionised components and a beam collector cup with a thermopile and a pressure sensor to characterise the resulting neutral atom beam. Energetic neutral atoms are created as a result of energy transfer through collisions between the accelerated ionized gas clusters and non-ionised gas atoms present along the beam path. This process causes the accelerated ionized gas clusters to become unstable and leads to the dissociation of bonds within the cluster until stability is restored. Careful optimisation of parameters allows converting most of the total energy originally imparted to the gas clusters into energy carried by the energetic neutral atoms. If the cluster is not fully dissociated, it has been shown that the original charge remains within a residual cluster. The ionized components from the main beam are removed using the electrostatic deflector, thus allowing only the dissociated neutral atoms to reach the target. The described setup allows combining both the GCIB and ANAB techniques to enable a wide range of modifications on surfaces, depending on the material and on the required surface finishing, with favourable sub-surface quality. Both GCIB and ANAB produce “lateral sputtering” behavior in which sputtered atoms are ejected preferentially at shallow angles relative to the target surface plane [9, 10]. The lateral sputtering effect results in an inherent surface smoothing action due to favored elimination of atoms from high features relative to removal from low areas. Lateral sputtering can be employed to reduce the rms roughness of most materials to well below one nm in the case of GCIB, and typically to as low as 0.1 nm in the case of ANAB. When GCIB bombardment is conducted at very high acceleration potentials, energy deposited at individual cluster ion impact sites can be sufficient to produce extreme instantaneous temperatures and associated spallation of minute volumes of vaporized target material from those impact

points, thereby resulting in surface texture of nanoscale dimensions. It is also worth noting that both the GCIB and the ANAB techniques are dry processes, i.e. not requiring the use of slurries which need to be carefully cleaned off after the polishing process.

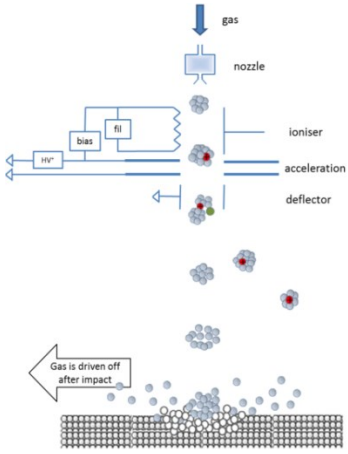

Fig. 1. Schematic of ANAB processing station.

3. Sample Preparation

3.1 GCIB and ANAB surface treatment

The GCIB and the ANAB techniques were applied to a set of ten 1 at-% Yb^{3+}-doped ceramic YAG substrates, each with a size of 24 mm x 24 mm x 7 mm, supplied by Konoshima Chemical (Japan) and polished on both square faces by Baikowski International (Japan) to an rms surface roughness of about 0.5 nm. Sample surfaces were characterised before and after processing using a Park model XE-70 atomic force microscope (AFM) run in non-contact mode with a NanoAndMore P/N: PPP-NCHR standard AFM tip, with a tip radius < 7 nm. 10 µm x 10 µm and 1 µm x 1 µm AFM scans of the surface of a sample before treatment are shown in Figs. 2(a) and 2(b), respectively, along with information on the peak-to-valley (PV) and the rms roughness (Rq) values. The AFM images clearly show typical polishing marks, along with protruding features, seen as white speckles in the image, due to particle contamination.

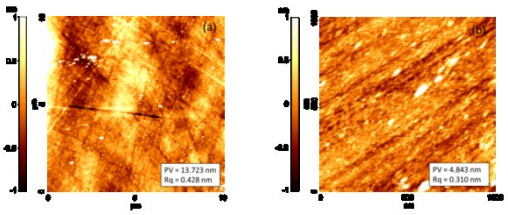

Fig. 2. 10 µm x 10 µm (a) and 1 µm x 1 µm (b) AFM surface image and statistics of an untreated sample (from [11]).

Both nano-texturing and polishing capabilities were investigated. To this end, a first set of 5 samples, further referred to as nano-textured samples, was GCIB treated aiming to achieve uniform surface nano-texturing. A second set of 5 samples, further referred to as polished samples, was treated to achieve angstrom-level surface smoothing.

3.1.1 Nano-texturing

The first set of samples was treated on both faces using the GCIB technique to achieve a nano-textured surface. Argon gas clusters were accelerated at 30 kV and each square centimetre of the sample was exposed for 40 seconds with a dose of $8 \cdot 10^{17}$ atoms. As shown in Figs. 3 and 4(a), the result was a uniform nano-texture in the form of undulations, a few nanometres high, characterised by an rms roughness of 0.923 nm.

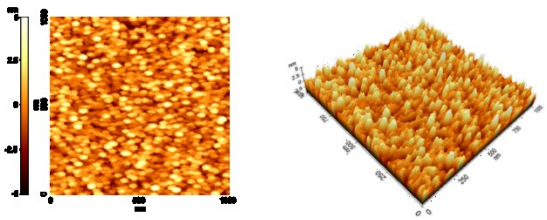

Fig. 3. 1 µm x 1 µm AFM surface image and 3D reconstruction of a nano-textured sample.

The two-dimensional surface roughness power spectral density (PSD) of the nano-textured surface, shown in Fig. 4(b), indicates a random distribution of surface undulations.

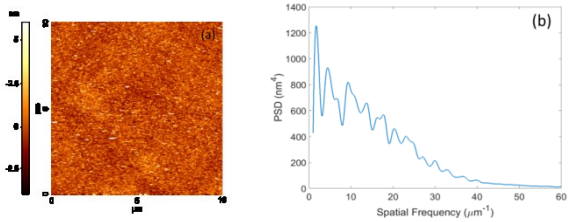

Fig. 4. 10 µm x 10 µm AFM image (a) and 2D surface roughness PSD of a nano-textured sample (b).

3.1.2 Angstrom-level polishing

The second set of samples was treated to achieve angstrom-level polishing through a two-stage process. The first stage consisted of a GCIB treatment, with the same processing parameters employed for the nano-texturing treatment. During the second stage, the sample was ANAB treated using argon neutral atoms accelerated to an average energy of 30 eV and exposing each square centimetre of the sample for 80 seconds with a dose of $4 \cdot 10^{18}$ atoms. The resulting surface quality is shown in Fig. 5. As a result of the processing, the rms surface roughness decreased from about 0.5 nm of the untreated substrates to 0.172 nm, showing a reduction by a factor of approximately three and a final roughness value comparable to the one achievable through super-polishing [12]. Polishing marks observed on supplied samples were completely removed as a result of the ANAB process.

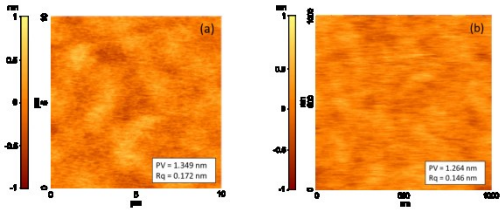

Fig. 5. 10 µm x 10 µm (a) and 1 µm x 1 µm (b) AFM surface image and statistics of an ANAB polished sample.

3.2 Coating deposition

After the GCIB/ANAB processes, samples were packaged in vacuum-tight containers designed to contact the samples only on the edges to minimise damage and contamination to the treated surfaces. In order to assess the LIDT of optical coatings on the treated substrates, multilayer SiO_2/Ta_2O_5 anti-reflective (AR) coatings were deposited on one of the treated surfaces for a number of samples, leaving the opposite surface uncoated. AR coatings, deposited by Laseroptik GmbH (Germany), were designed for 99.75% transmission at both 939 nm and 1030 nm. Prior to coating, all samples underwent inspection and cleaning following the procedure described in [13]. Two possible deposition techniques, widely applied to optical components for high energy laser systems, were used in this study, namely Ion Assisted Deposition (IAD) and Ion Beam Sputtering (IBS). Each coating technique was applied to both polished and nano-textured samples during the same coating run.

4. LIDT Testing Methods

Both 1000-on-1 and raster scanning LIDT tests in the nanosecond regime were performed at ambient conditions at the Lidaris facility in Vilnius (Lithuania) in accordance with the ISO 21254-2 and the ISO 21254-3 standards, respectively. A 1064 nm Nd:YAG InnoLas SplitLight Hybrid Laser operating on a single longitudinal mode with a pulsed width of 10.2 ± 0.5 ns (measured at full width at half maximum) and a pulse repetition rate of 100 Hz was used. LIDT under 1064 nm irradiation is representative of the LIDT under 1030 nm irradiation due to the similar electric field distribution within the coatings at these two wavelengths. In the case of 1000-on-1 tests, the beam at the sample surface showed a Gaussian spatial profile with a $1/e^2$ diameter of 250 μm (averaged over 64 pulses). 1000-on-1 LIDT values were retrieved by nonlinear fit to 0% of damage probability. Complementary information on rear surface damage was also extracted during the front surface LIDT measurements. This was achieved by monitoring damage onset to the back surface resulting from beam propagation through the sample. It is worth nothing that, while this measurement is useful to characterise the behaviour of the whole sample under laser irradiation, it does not provide the actual LIDT of the back surface because the beam was focused on the front surface.

Raster scanning tests were carried out on a larger area compared to the one probed in the 1000-on-1 tests to increase the confidence that defects, which limit the performance of large aperture optics, were being irradiated. Samples were tested on a 1 cm^2 square region using the same setup employed for the 1000-on-1 tests. All irradiation parameters were kept the same, with the exception of the spot $1/e^2$ diameter at the sample surface, which was increased to 972.7 ± 3.7 μm. Each site was irradiated with 1000 pulses at a fluence level which was kept constant throughout the raster scanning test. All samples were initially tested at a fluence of 3.5 J/cm^2. If no damage was detected over the entire testing area, the raster scanning tests were repeated at higher fluence levels. Test sites were equally spaced by 485 μm and arranged according to a hexagonal geometry distribution, thus achieving 50% overlap between adjacent sites. Both in the case of the 1000-on-1 and of the raster scanning tests, occurrence and position of damage were monitored both during and after each test.

5. Experimental results and discussion

5.1 LIDT of uncoated samples

Resilience of treated surfaces to laser irradiation in the nanosecond regime was characterised and compared against that of untreated samples. 1000-in-1 LIDT results are summarised in Table 1.

Table 1. Front surface and back surface 1000-on-1 LIDT values of uncoated samples.

Sample	Front surface LIDT (J/cm^2)	Back surface threshold (J/cm^2)
Untreated	9.5 ± 2.2	10.4 ± 2.7
Nano-textured	13.7 ± 2.2	11.9 ± 1.8
Polished	18.2 ± 2.2	16.2 ±2.0

The LIDT values for untreated, nano-textured and polished samples are 9.5 J/cm^2, 13.7 J/cm^2 and 18.2 J/cm^2, respectively, with an error of ± 2.2 J/cm^2. Results show an improvement in the LIDT for both nano-textured and polished samples compared to untreated Yb:YAG, with polished Yb:YAG exhibiting the best performance. These results show that damage resilience of uncoated substrates is increased as a result of the GCIB and the ANAB treatments, possibly due to an improvement in the sub-surface quality compared to untreated substrates.

5.1 LIDT of uncoated samples

Coated samples were tested under the same testing parameters employed for uncoated substrates. Table 2 and Table 3 report the 1000-on-1 LIDT results for IAD and IBS coatings deposited on nano-textured and polished substrates, respectively, along with the LIDT of uncoated substrates for comparison.

Table 2. 1000-on-1 LIDT results of nano-textured samples, both uncoated and coated.

Sample	Front surface LIDT (J/cm^2)	Back surface threshold (J/cm^2)
Uncoated	13.7 ± 2.2	11.9 ± 1.8
IAD-coated	12.3 ± 2.3	12.3 ± 1.9
IBS-coated	NA[a]	13.2 ± 1.9

[a]The lowest fluence at which damage occurred on the front surface after 1000 pulses was 32.4 J/cm^2.

Table 3. 1000-on-1 LIDT results of polished samples, both uncoated and coated.

Sample	Front surface LIDT (J/cm^2)	Back surface threshold (J/cm^2)
Uncoated	18.2 ± 2.2	16.2 ± 2.0
IAD-coated	7.5 ± 1.5	15.6 ± 2.5
IBS-coated	11.2 ± 2.6	15.2 ± 3.7

In the case of polished substrates, both IAD and IBS coated samples showed less resilience to laser irradiation compared to uncoated substrates, with a front surface LIDT of 7.5 J/cm^2 and 11.2 J/cm^2 respectively. The LIDT of IAD coatings deposited on nano-textured samples was 12.3 J/cm^2, higher than the LIDT of the IAD coating deposited on the polished substrate and comparable with that of the uncoated nano-textured substrate. On the other hand, IBS coatings deposited on nano-textured samples showed an extremely high damage resilience, which prevented the determination of the LIDT. Indeed, on most sites, damage occurred on the rear uncoated surface first and irradiation had to be stopped to prevent damage growth and consequent creation of ablation products which would affect the measurement. The lowest fluence at which damage occurred on the front surface after 1000 pulses was 32.4 J/cm^2. As evident from Table 2, the LIDT of the rear uncoated surface remained comparable to that of the other samples, thus giving further assurance on the correctness of the measurement. Both IAD and IBS coatings deposited on nano-textured substrates exhibited higher resilience to laser irradiation than coatings deposited on polished substrates. This indicates that, while a very low roughness improves the LIDT of uncoated substrates, surface nano-texturing allows to achieve a higher LIDT if the surface is coated.

Raster scanning tests, as described in Section 4, were carried out on a batch of four coated samples. Samples were tested at increasing fluence levels of 3.5 J/cm^2, 5 J/cm^2, 7.5 J/cm^2 and 10 J/cm^2. If no damage was observed on the whole tested area (pass), the laser fluence was increased to the subsequent level until damage of the surface was observed (fail). Raster scanning test results are summarised in Table 4.

Table 4. Raster scanning results of nano-textured and polished coated samples.

Surface Processing	Coating Technique	3.5 ± 0.5 J/cm^2	5.0 ± 0.7 J/cm^2	7.5 ± 1.1 J/cm^2	10.0 ± 1.3 J/cm^2
Nano-structured	IAD-coated	*Pass*	*Pass*	*Pass*	*Pass*
Nano-structured	IBS-coated	*Pass*	*Pass*	*Pass*	*Pass*
Polished	IAD-coated	*Pass*	*Pass*	*Pass*	*Fail*
Polished	IBS-coated	*Pass*	*Pass*	*Pass*	*Fail*

In the case of polished substrates, both IAD and IBS coated substrates suffered from damage during the raster scanning test at a fluence of 10 J/cm^2. On the contrary, both nano-textured samples did not sustain damage in any of the raster scanning tests. Further raster scanning tests at fluence levels above 10J/cm^2 were prevented by lack of un-irradiated space on the sample surface.

Both 1000-on-1 LIDT and raster scanning test results support the evidence that the GCIB and the ANAB surface treatment techniques are suitable for high-energy laser applications. A higher resilience to laser irradiation was observed for nano-textured samples in both testing regimes. Since for a given coating technique all substrates (both polished and nano-textured) were coated in the same coating run, no variations in coating characteristics are expected. Therefore, observed differences in performance between polished and nano-textured substrates can be ascribed to the characteristics of the substrate and/or of the interface between the coating and the substrate. Differences in resilience to laser irradiation between coatings deposited on polished and nano-textured substrates show that, in the cases under investigation, the characteristics of the interface between substrate and coating might represent the main factor influencing test outcomes. A possible explanation for the increase in the LIDT observed for coatings deposited on nano-textured samples is an improvement in the coating-substrate interface quality, possibly due to higher coating adhesion facilitated by the surface nano-texturing. Further research will be required to validate this hypothesis.

6. Conclusion

We investigated the GCIB and the ANAB techniques as alternatives to conventional surface finishing techniques for ceramic Yb:YAG. We demonstrated that these techniques allow highly controllable and flexible surface finishing, enabling both angstrom-level polishing and uniform nano-texturing. To the best of our knowledge, this is the first time that the GCIB and the ANAB techniques are proposed as surface treatments for optical ceramic Yb:YAG. Characterisation of the LIDT of both uncoated and coated substrates was carried out. We observed a improvement in the LIDT for both polished and nano-textured uncoated substrates compared to untreated substrates, possibly due to an improvement in the sub-surface quality. Both 1000-on-1 and raster scanning tests carried out on coated substrates demonstrate that the GCIB and the ANAB techniques are suitable for the processing of ceramic Yb:YAG substrates for high-energy laser applications. Higher resilience to laser irradiation was observed in the case of nano-textured coated substrates, suggesting that surface nano-texturing brings about an improvement in the quality of the interface between the coating and the substrate, possibly due to better adhesion of the coatings to the substrate.

Acknowledgements

MDV is supported by the Engineering and Physical Sciences Research Council (EPSRC) through the Centre for Doctoral Training in Applied Photonics.

References

[1] S. P. D. Mangles, C. D. Murphy, Z. Najmudin, A. G. R. Thomas, J. L. Collier, A. E. Dangor, E. J. Divall, P. S. Foster, J. G. Gallacher, C. J. Hooker, D. A. Jaroszynski, A. J. Langley, W. B. Mori, P. A. Norreys, F. S. Tsung, R. Viskup, B. R. Walton, and K. Krushelnick, "Monoenergetic beams of relativistic electrons from intense laser–plasma interactions," Nature **431**, 535-538 (2004).

[2] H. Schwoerer, S. Pfotenhauer, O. Jäckel, K. Amthor, B. Liesfeld, W. Ziegler, R. Sauerbrey, K. W. D. Ledingham, and T. Esirkepov, "Laser-plasma acceleration of quasi-monoenergetic protons from microstructured targets," Nature **439**, 445–448 (2006).

[3] S. Kneip, S. R. Nagel, C. Bellei, N. Bourgeois, A. E. Dangor, A. Gopal, R. Heathcote, S. P. D. Mangles, J. R. Marques, A. Maksimchuk, P. M. Nilson, K. Ta Phuoc, S. Reed, M. Tzoufras, F. S. Tsung, L. Willingale, W. B. Mori, A. Rousse, K. Krushelnick, and Z. Najmudin, "Observation of synchrotron radiation from electrons accelerated in a petawatt-laser-generated plasma cavity," Phys. Rev. Lett. **100**, 105006 (2008).

[4] M. Dunne, "A high-power laser fusion facility for Europe," Nat. Phys. **2**, 2-5 (2006).

[5] G. Miller, E. Moses, and C. Wuest, "The national ignition facility," Opt. Eng. **43**, 2841–2853 (2004).

[6] P. D. Mason, M. Fitton, A. Lintern, S. Banerjee, K. Ertel, T. Davenne, J. Hill, S. P. Blake, P. J. Phillips, T. J. Butcher, J. M. Smith, M. De Vido, R. J. S. Greenhalgh, C. Hernandez-Gomez, and J. L. Collier, "Scalable design for a high energy cryogenic gas cooled diode pumped laser amplifier," Applied Optics **54**(13), 4227-4238 (2015).

[7] A. A. Manenkov, "Fundamental mechanisms of laser-induced damage in optical materials: today's state of understanding and problems," Optical Engineering **53**(1), 010901 (2014).

[8] M. F. Koldunov, and A. A. Manenkov, "Theory of laser-induced inclusion-initiated damage in optical materials," Optical Engineering **51**(12), 121811-1 (2012).

[9] I. Yamada, J. Matsuo, N. Toyoda, A. Kirkpatrick, "Materials processing by gas cluster ion beams" Mat. Sci. Eng. R: Reports **34**(6), 231-295 (2001).

[10] A. Kirkpatrick, S. Kirkpatrick, M. Walsh, S. Chau, M. Mack, S. Harrison, R. Svrluga, J. Khoury, "Investigation of accelerated neutral atom beams created from gas cluster ion beams." Nuclear Instruments and Methods in Physics Research Section B: Beam Interactions with Materials and Atoms **307**, 281-289 (2013).

[11] M. De Vido, "Impact of GCIB and ANAB surface treatments on the LIDT of ceramic Yb:YAG," STFC Data Repository (2017), http://dx.doi.org/10.5286/edata/2.

[12] C. J. McHargue, and W. B. Snyder Jr. "Surface modification of sapphire for IR window application," SPIE's 1993 International Symposium on Optics, Imaging, and Instrumentation, 135-142 (1993).

[13] Laseroptik GmbH, http://www.laseroptik.de/en/customer-service/cleaning-of-substrates.